Supplement of Weather Clim. Dynam., 6, 841–862, 2025
https://doi.org/10.5194/wcd-6-841-2025-supplement

Supplement of

Assessing stratospheric contributions to subseasonal predictions of precipitation after the 2018 sudden stratospheric warming from the Stratospheric Nudging And Predictable Surface Impacts (SNAPSI) project

Ying Dai et al.

Correspondence to: Ying Dai (yd385@cornell.edu)

Contents of this file

1. Figures S1-S19

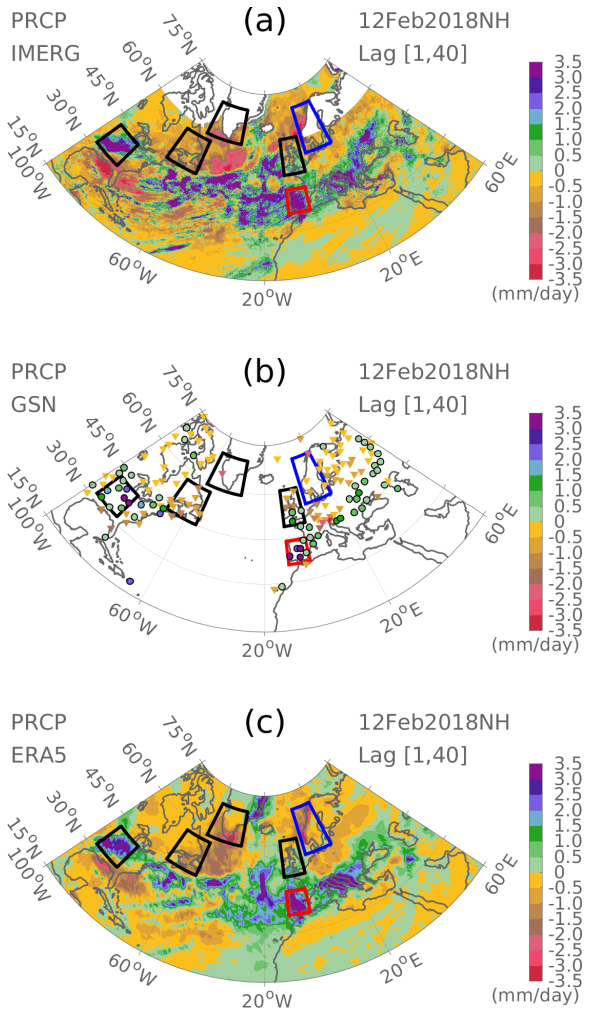

Figure S1. As in Figure 1 of the manuscript, but for precipitation anomalies averaged over lag days [1,40] relative to the SSW onset date.

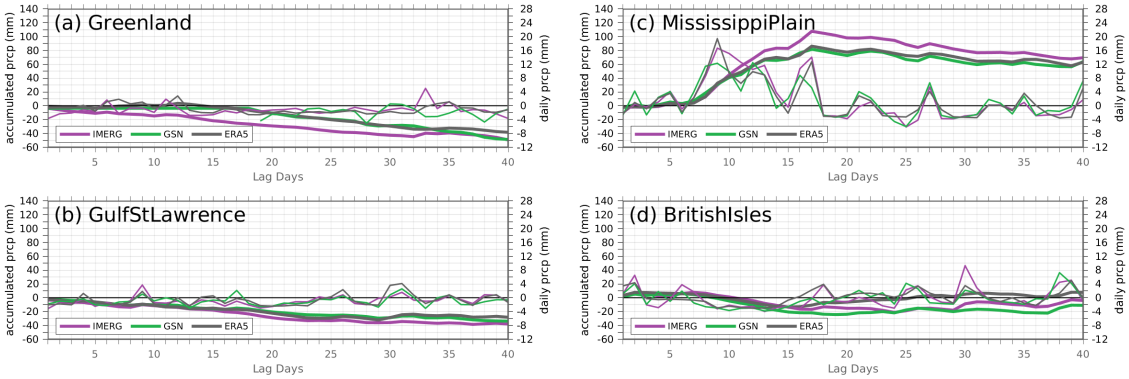

Figure S2. As in Figure 2 of the manuscript, but for precipitation anomalies averaged over (a) Greenland, (b) Gulf St Lawrence, (c) Mississippi Plain, and (d) British lsles. These four domains are indicated by the four black boxes in Figure 1 of the manuscript.

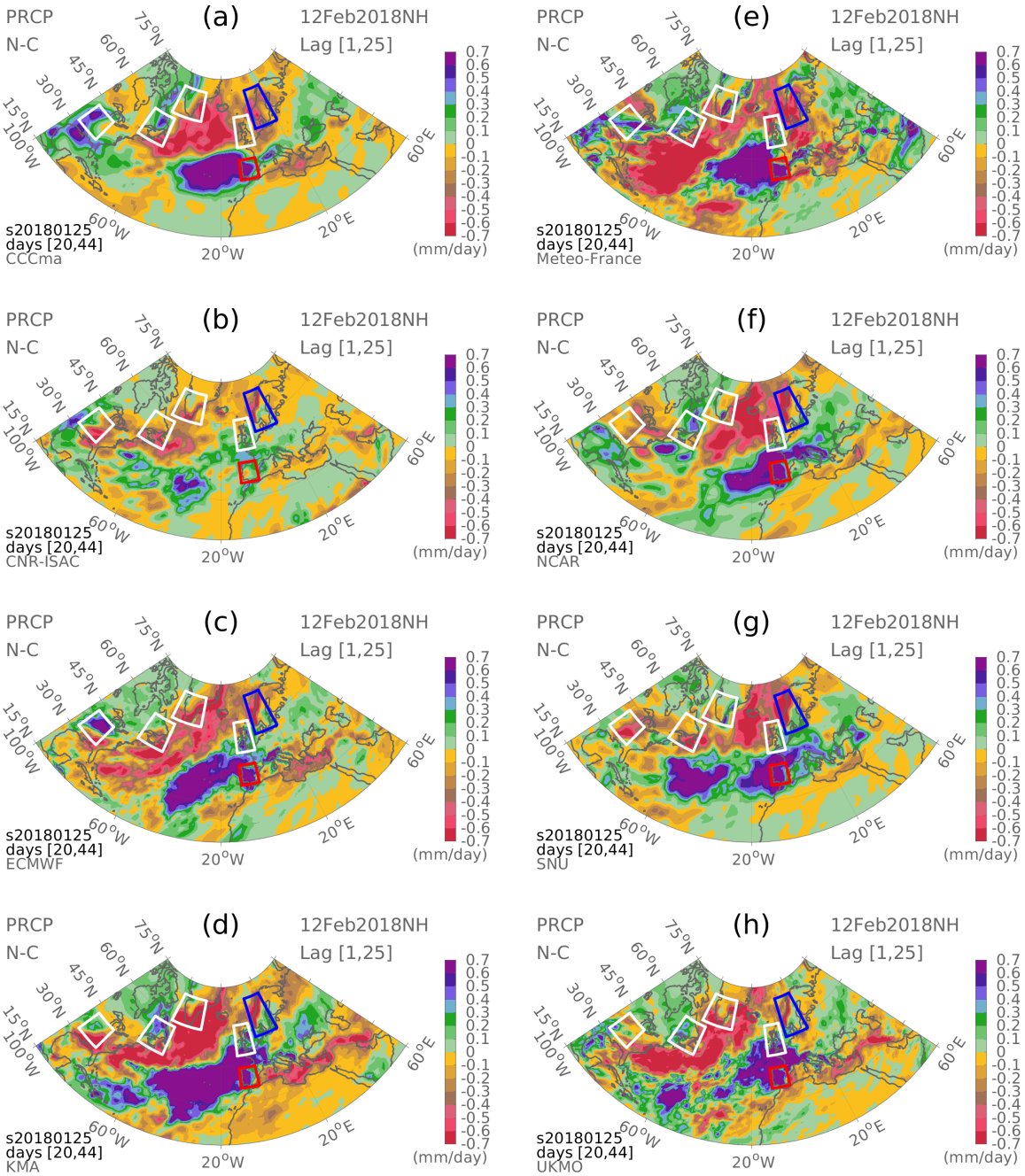

Figure S3. Precipitation anomalies averaged over lag days [1,25] relative to the SSW onset date from the early nudged ensemble by each of the eight models. For the early nudged ensemble, every single model captured the observed 'Wet Iberia and Dry Scandinavia' pattern.

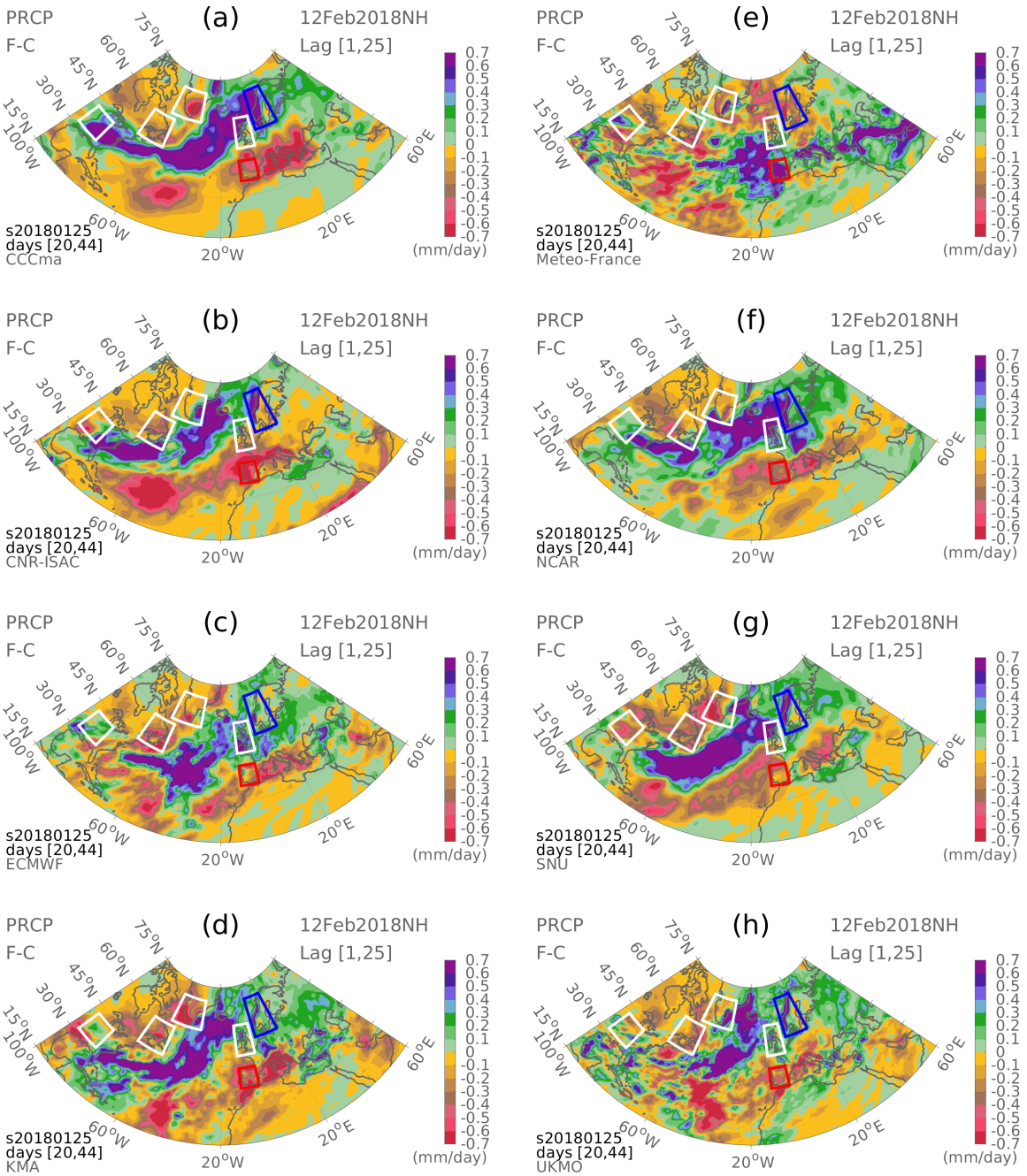

Figure S4. Precipitation anomalies averaged over lag days [1,25] relative to the SSW onset date from the early free ensemble by each of the eight models. For the early free ensemble, CNRM-CM61 is the only model that captured the observed 'Wet Iberia and Dry Scandinavia' pattern (panel e). By contrast, all of the other models predicted a 'Dry Iberia and Wet Scandinavia' pattern.

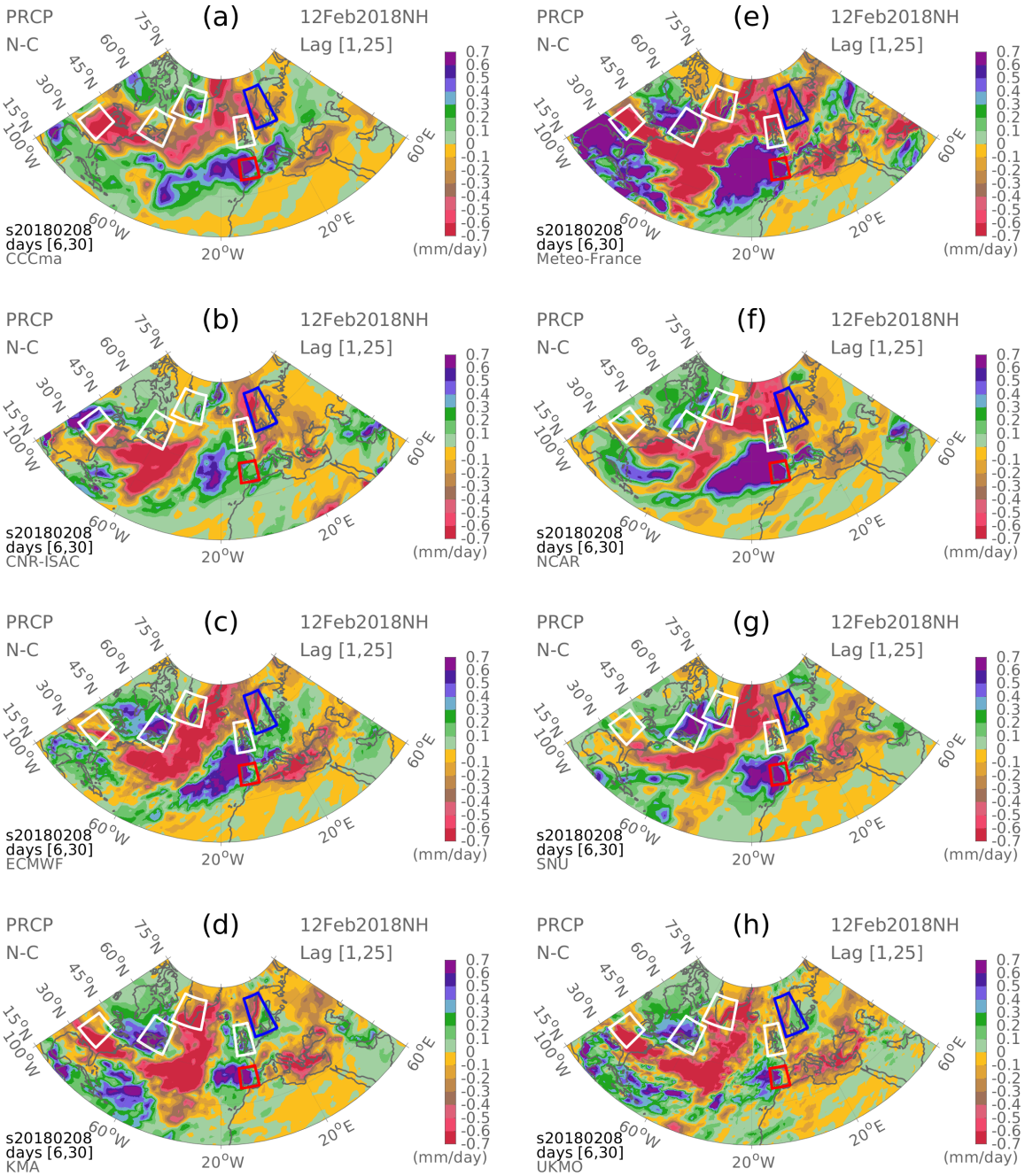

Figure S5. Precipitation anomalies averaged over lag days [1,25] relative to the SSW onset date from the late nudged ensemble by each of the eight models. For the late nudged ensemble, every single model captured the observed 'Wet Iberia and Dry Scandinavia' pattern.

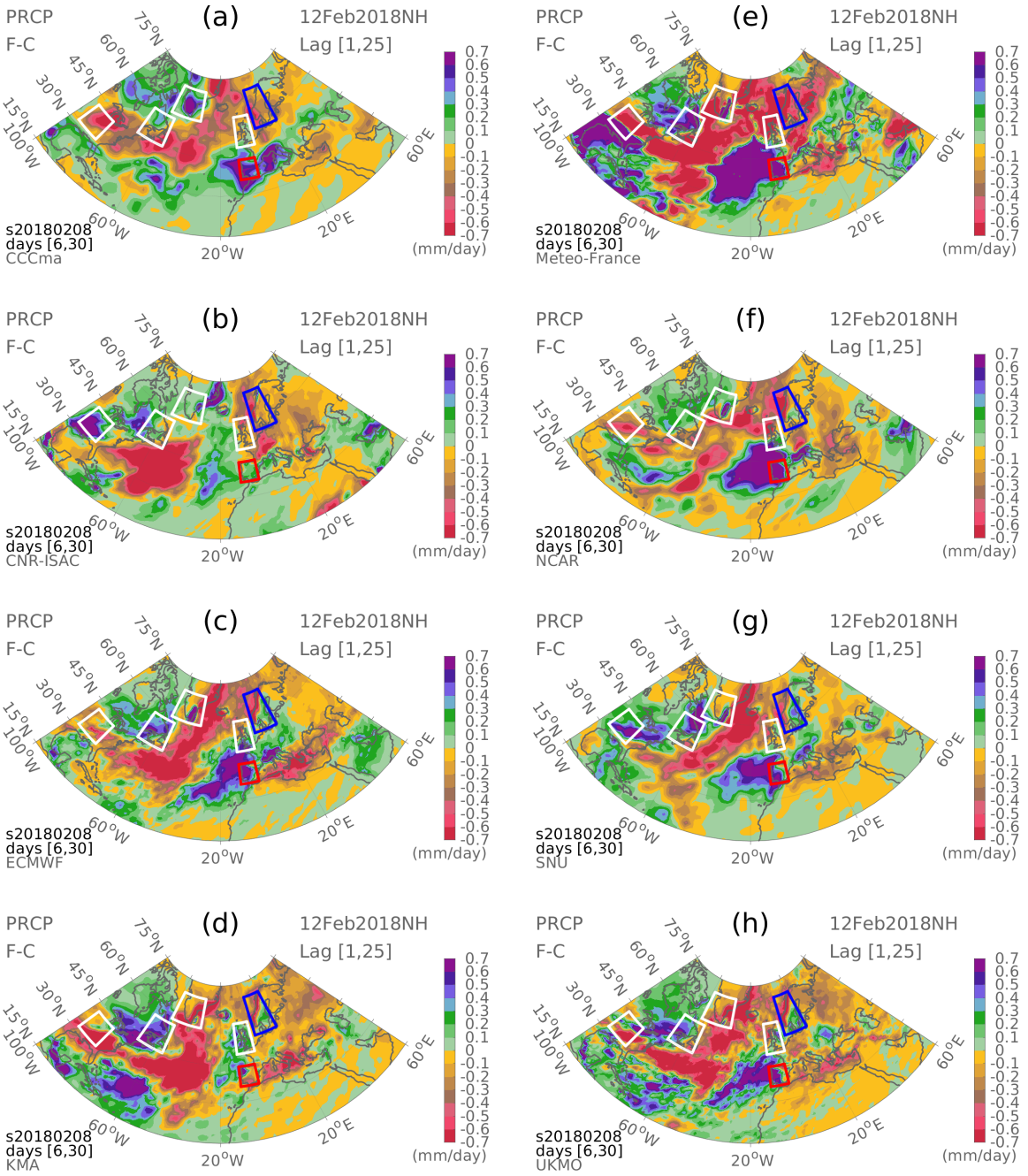

Figure S6. Precipitation anomalies averaged over lag days [1,25] relative to the SSW onset date from the late free ensemble by each of the eight models. For the late free ensemble, most models captured the observed 'Wet Iberia and Dry Scandinavia' pattern, with GloSea6-GC32 being the only model that failed to capture the 'Wet Iberia' signal (panel d).

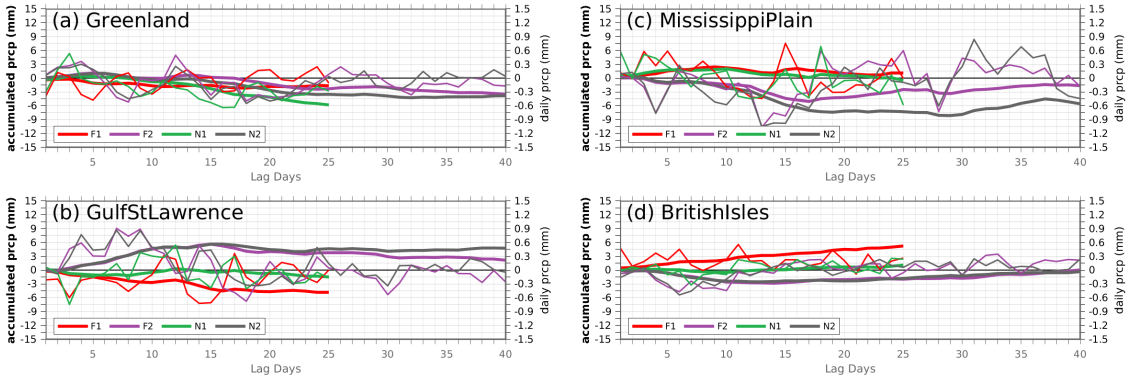

Figure S7. As in Figure 4 of the manuscript, but for precipitation anomalies averaged over (a) Greenland, (b) Gulf St Lawrence, (c) Mississippi Plain, and (d) British lsles. These four domains are indicated by the four white boxes in Figure 3 of the manuscript.

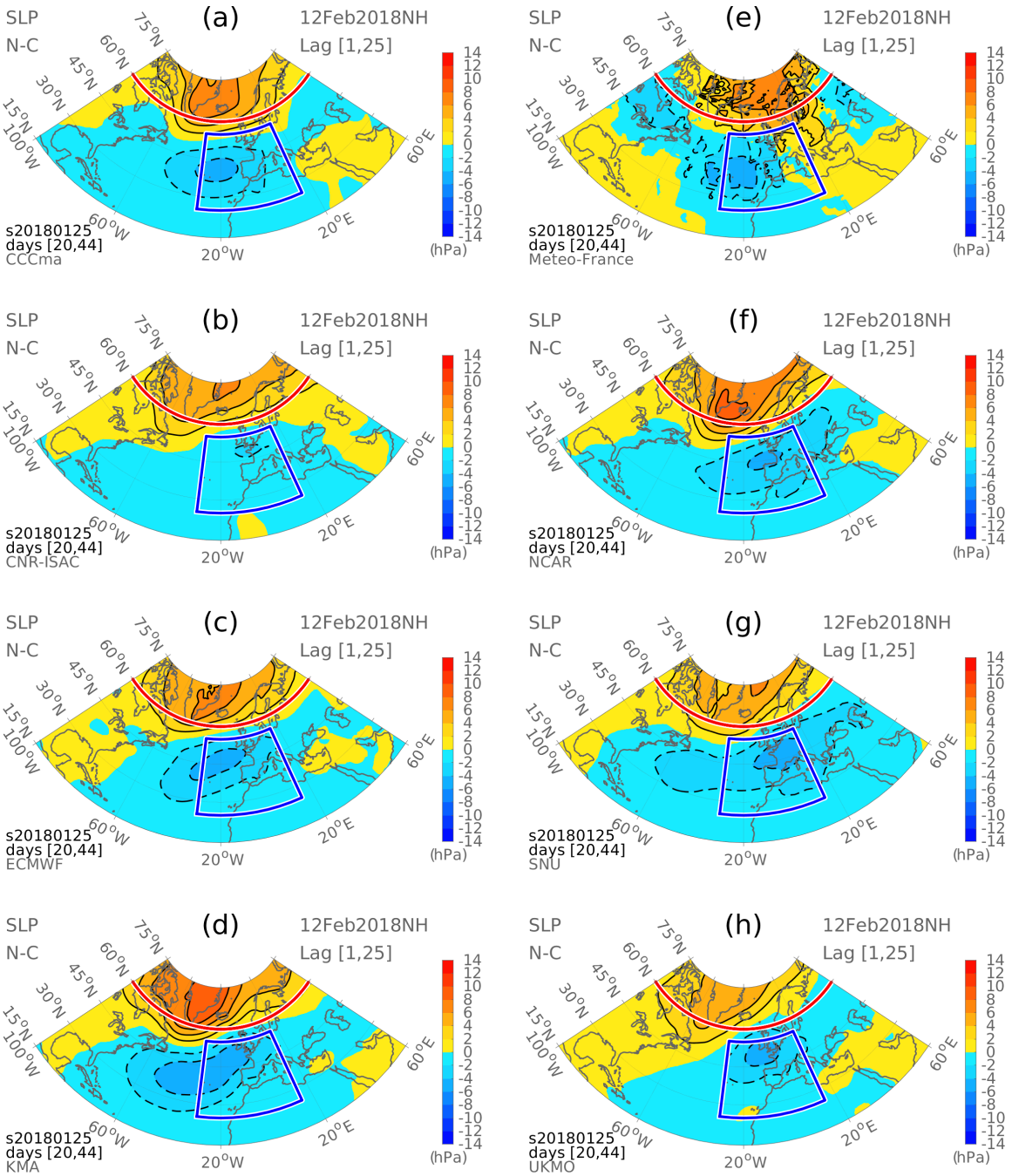

Figure S8. SLP anomalies averaged over lag days [1,25] relative to the SSW onset date from the early nudged ensemble by each of the eight models. For the early nudged ensemble, every single model captured the observed negative NAO-like SLP pattern.

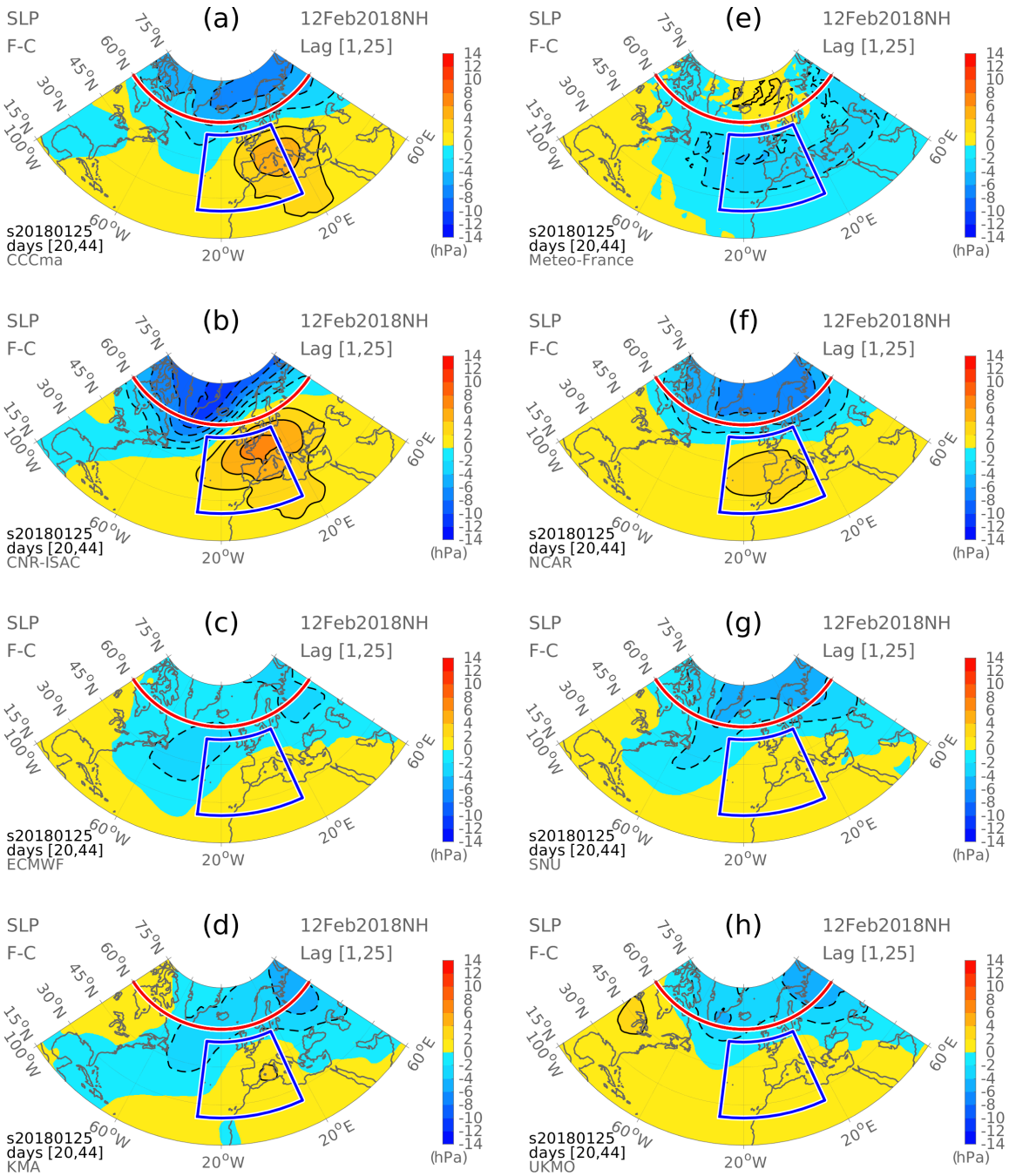

Figure S9. SLP anomalies averaged over lag days [1,25] relative to the SSW onset date from the early free ensemble by each of the eight models. For the early free ensemble, CNRM-CM61 is the only model that captured the observed negative NAO-like SLP pattern (panel e). By contrast, all of the other models predicted a positive NAO-like SLP pattern.

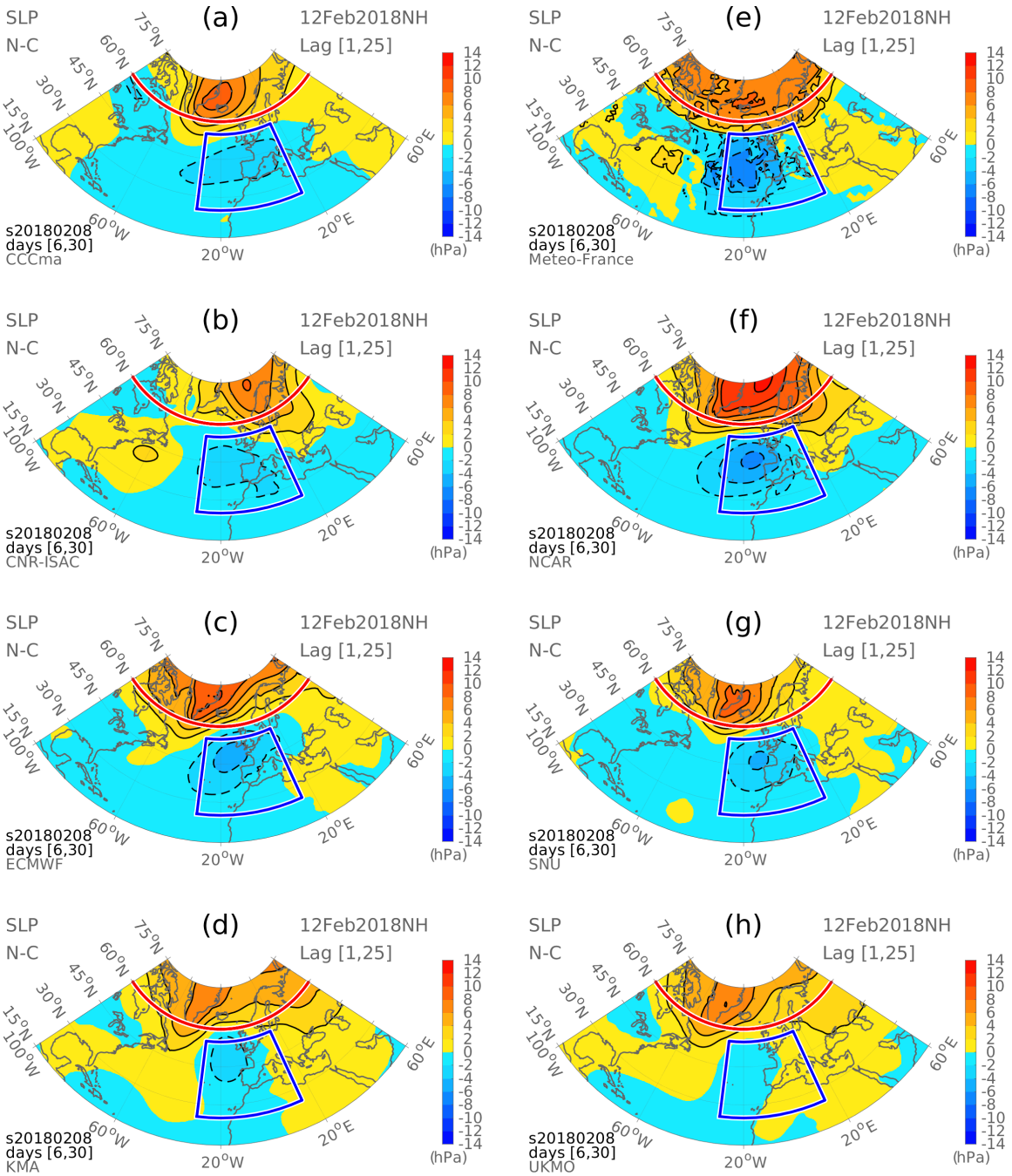

Figure S10. SLP anomalies averaged over lag days [1,25] relative to the SSW onset date from the late nudged ensemble by each of the eight models. For the late nudged ensemble, every single model captured the observed negative NAO-like SLP pattern.

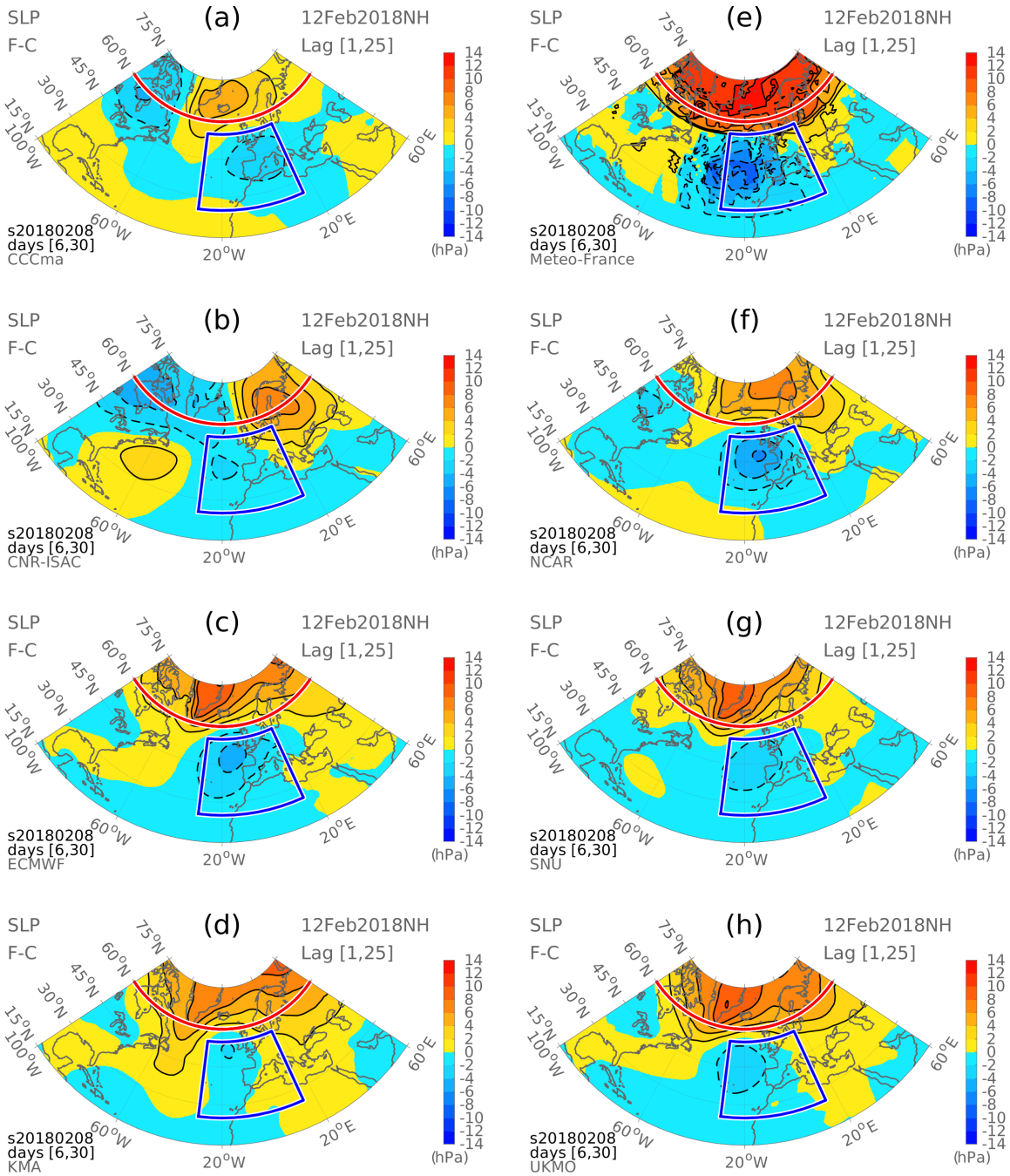

Figure S11. SLP anomalies averaged over lag days [1,25] relative to the SSW onset date from the late free ensemble by each of the eight models. For the late free ensemble, every single model captured the observed negative NAO-like SLP pattern.

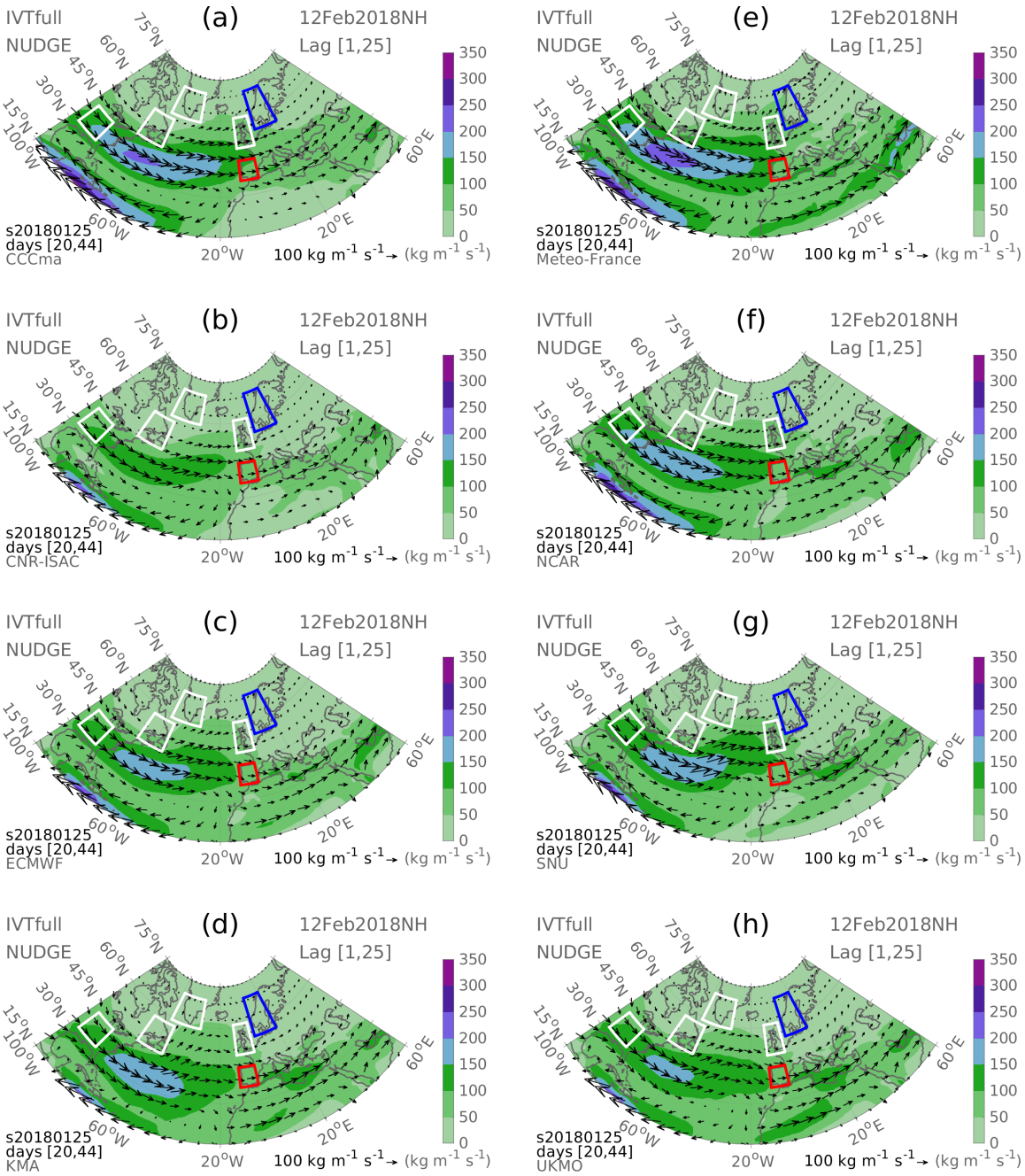

Figure S12. Vertically integrated water vapor transport (IVT) field (shadings) and water vapor flux (vector) averaged over lag days [1,25] relative to the SSW onset date from the early nudged ensemble by each of the eight models.

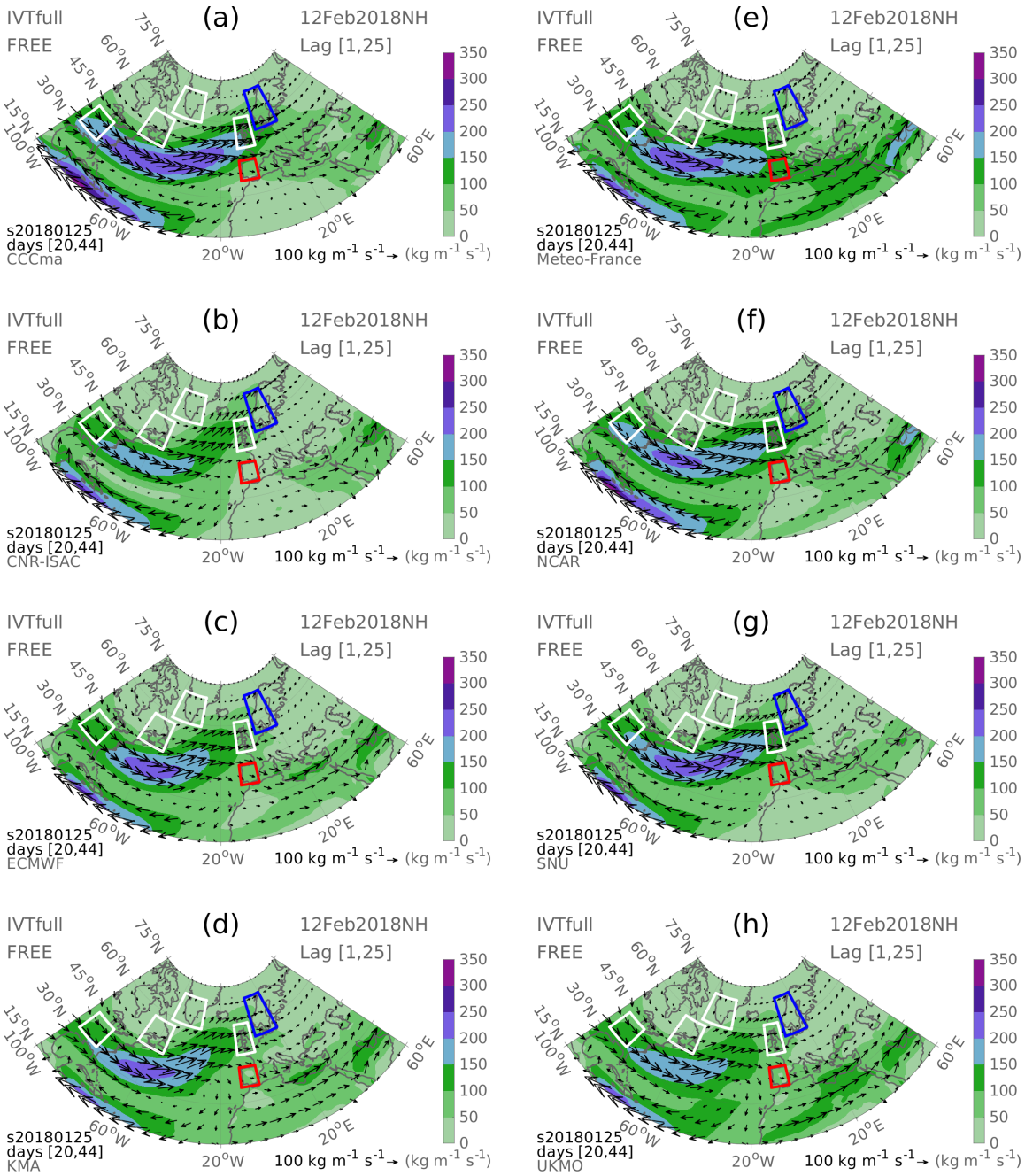

Figure S13. Vertically integrated water vapor transport (IVT) field (shadings) and water vapor flux (vector) averaged over lag days [1,25] relative to the SSW onset date from the early free ensemble by each of the eight models.

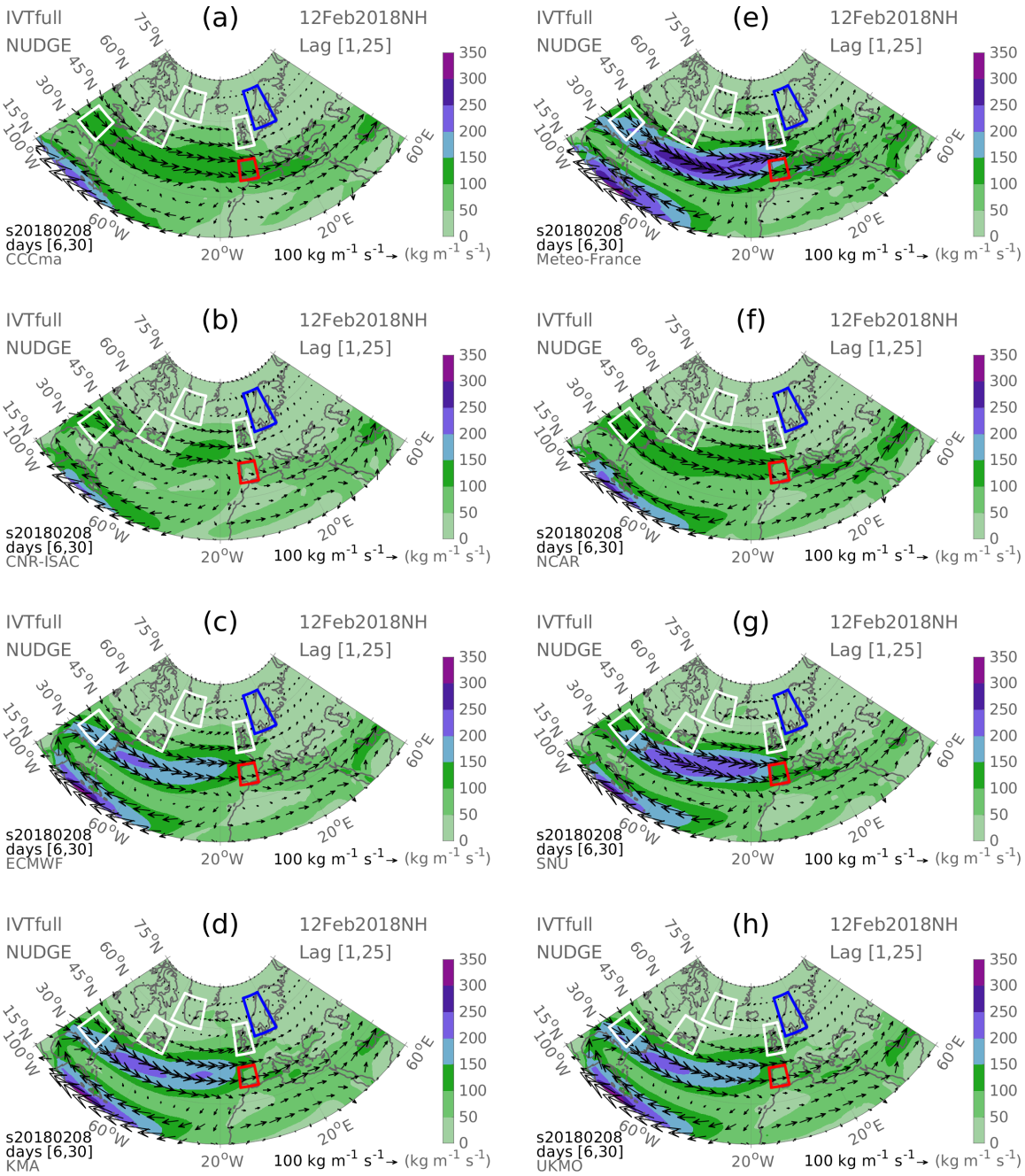

Figure S14. Vertically integrated water vapor transport (IVT) field (shadings) and water vapor flux (vector) averaged over lag days [1,25] relative to the SSW onset date from the late nudged ensemble by each of the eight models.

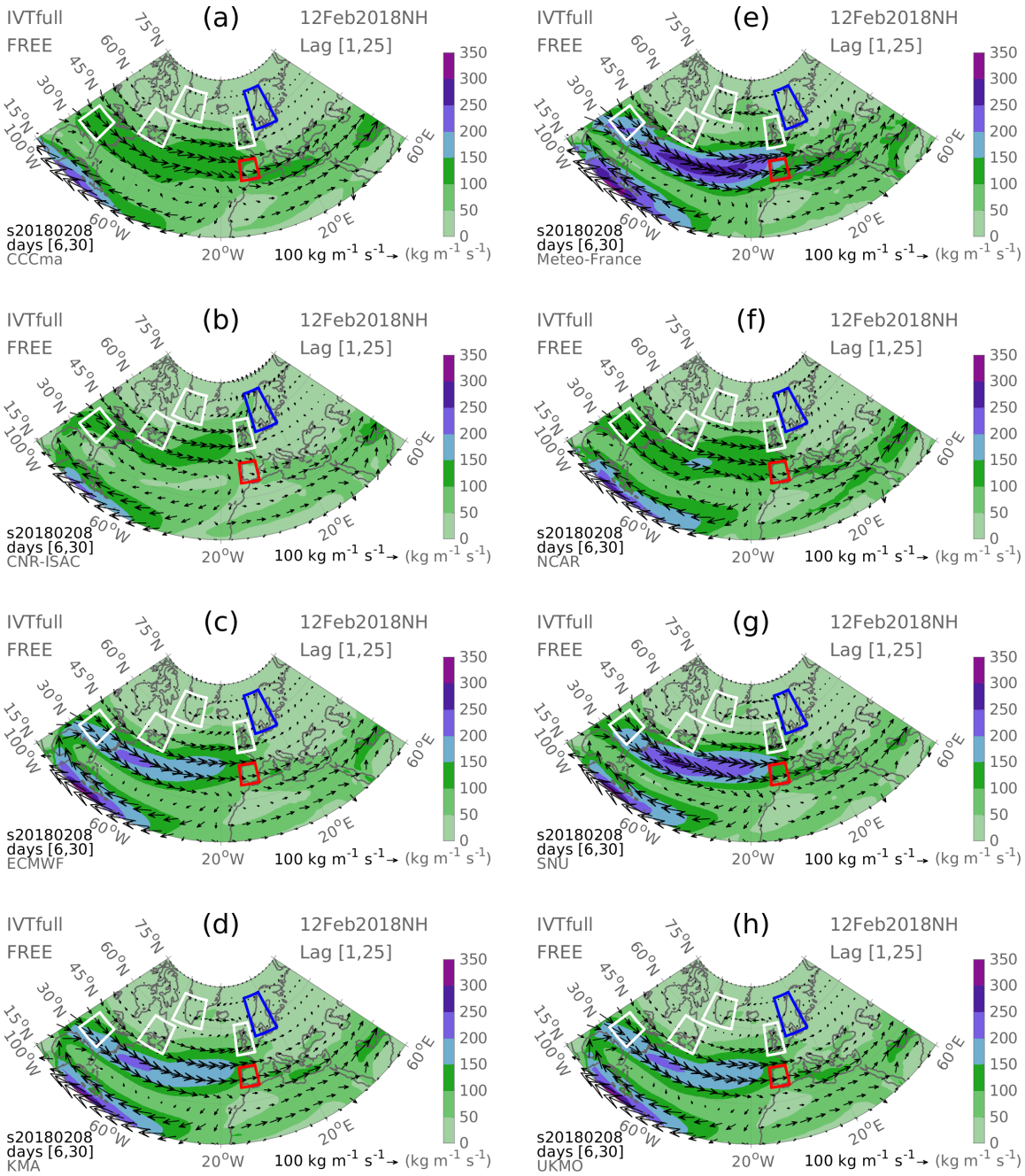

Figure S15. Vertically integrated water vapor transport (IVT) field (shadings) and water vapor flux (vector) averaged over lag days [1,25] relative to the SSW onset date from the late free ensemble by each of the eight models.

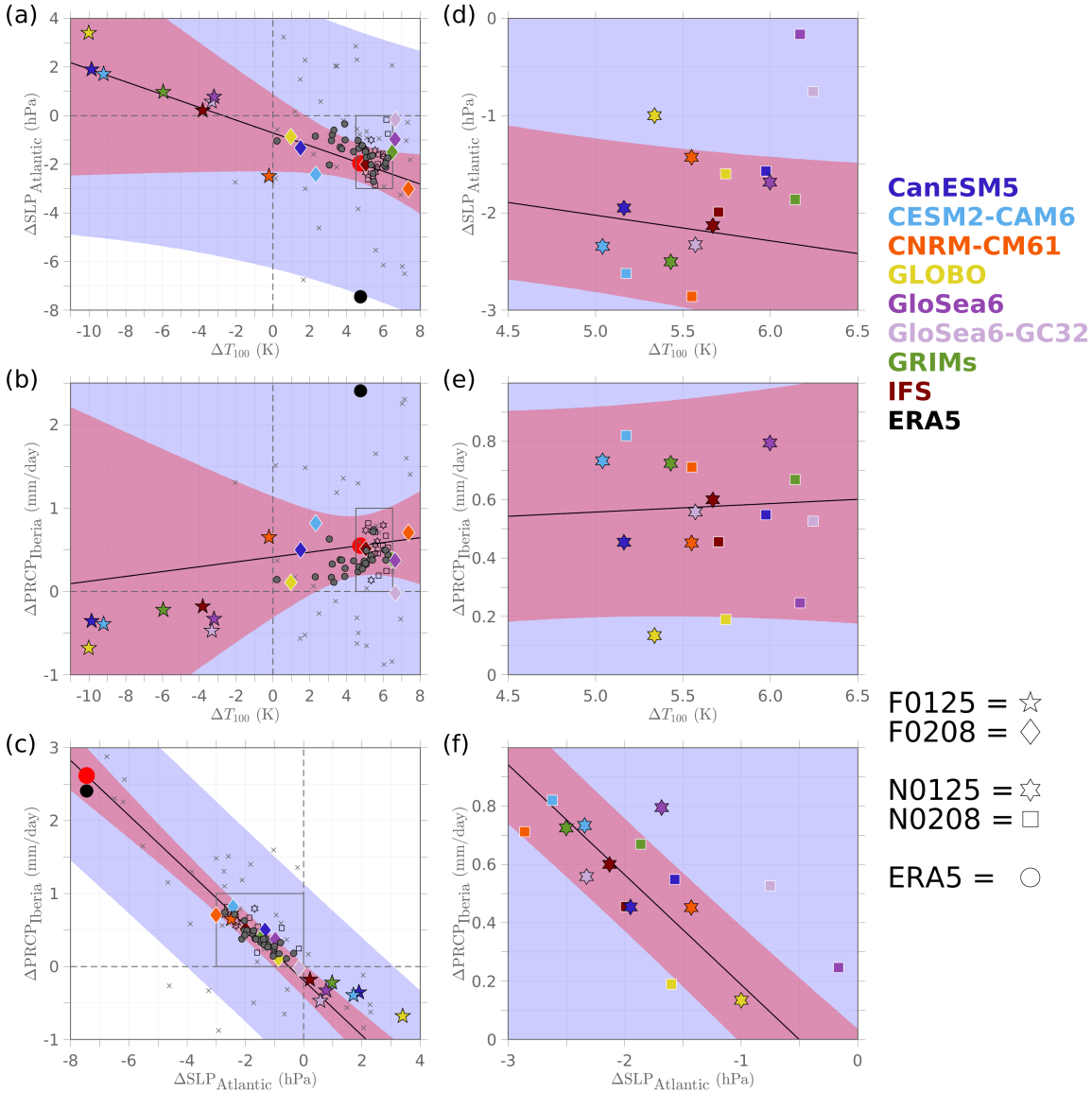

Figure S16. As in Figure 7 of the manuscript, but with the addition of 28 gray dots to illustrate results from 28 CMIP6 models in panels a-c. Each gray dot represents an individual CMIP6 model. For each CMIP6 model, the composite-averaged anomalies based on all SSW events available in that model are shown. See Dai et al. (2024) for more details of the 28 CMIP6 models and the number of SSW events in each of them.

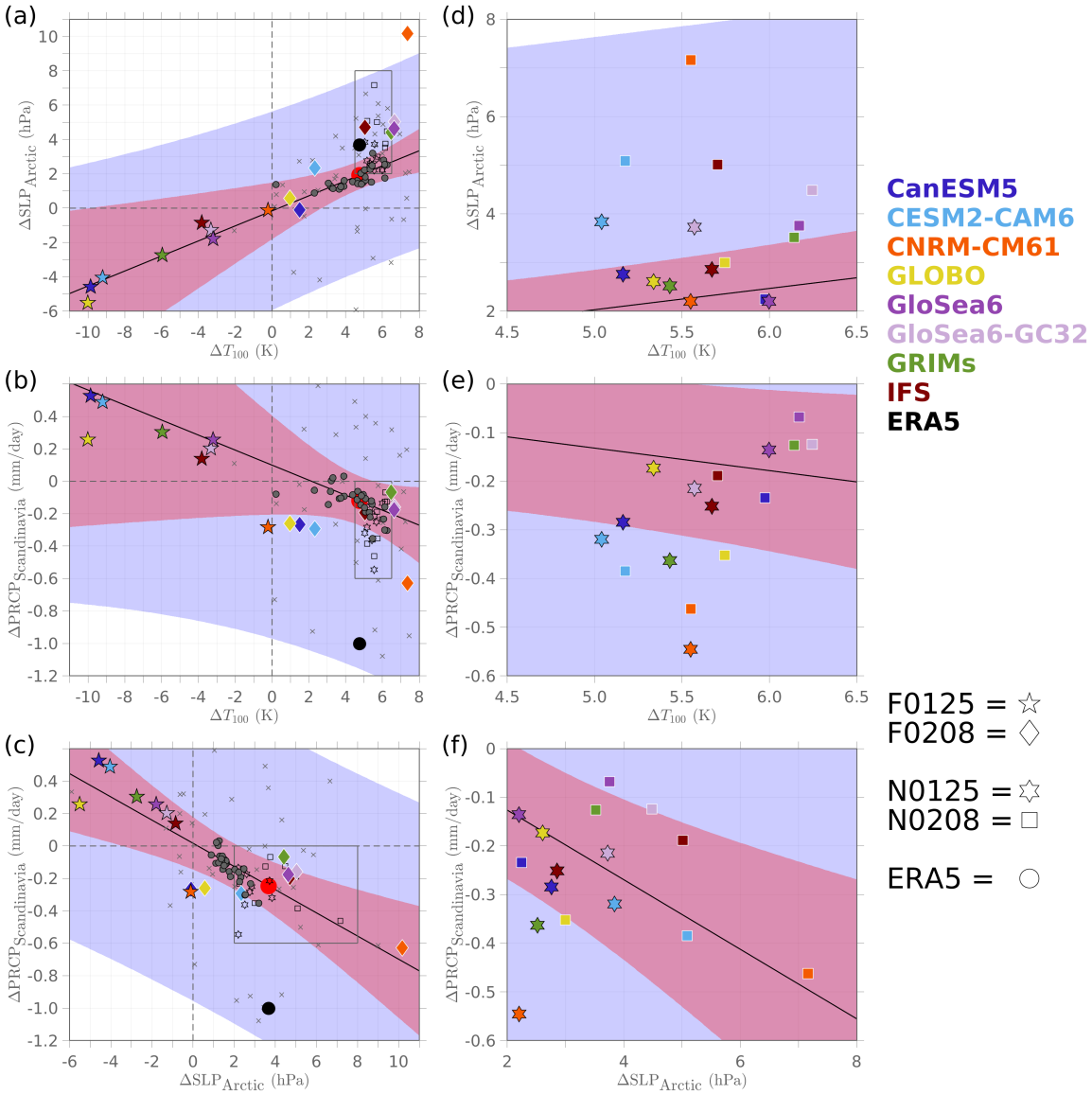

Figure S17. As in Figure 8 of the manuscript, but with the addition of 28 gray dots to illustrate results from 28 CMIP6 models in panels a-c.

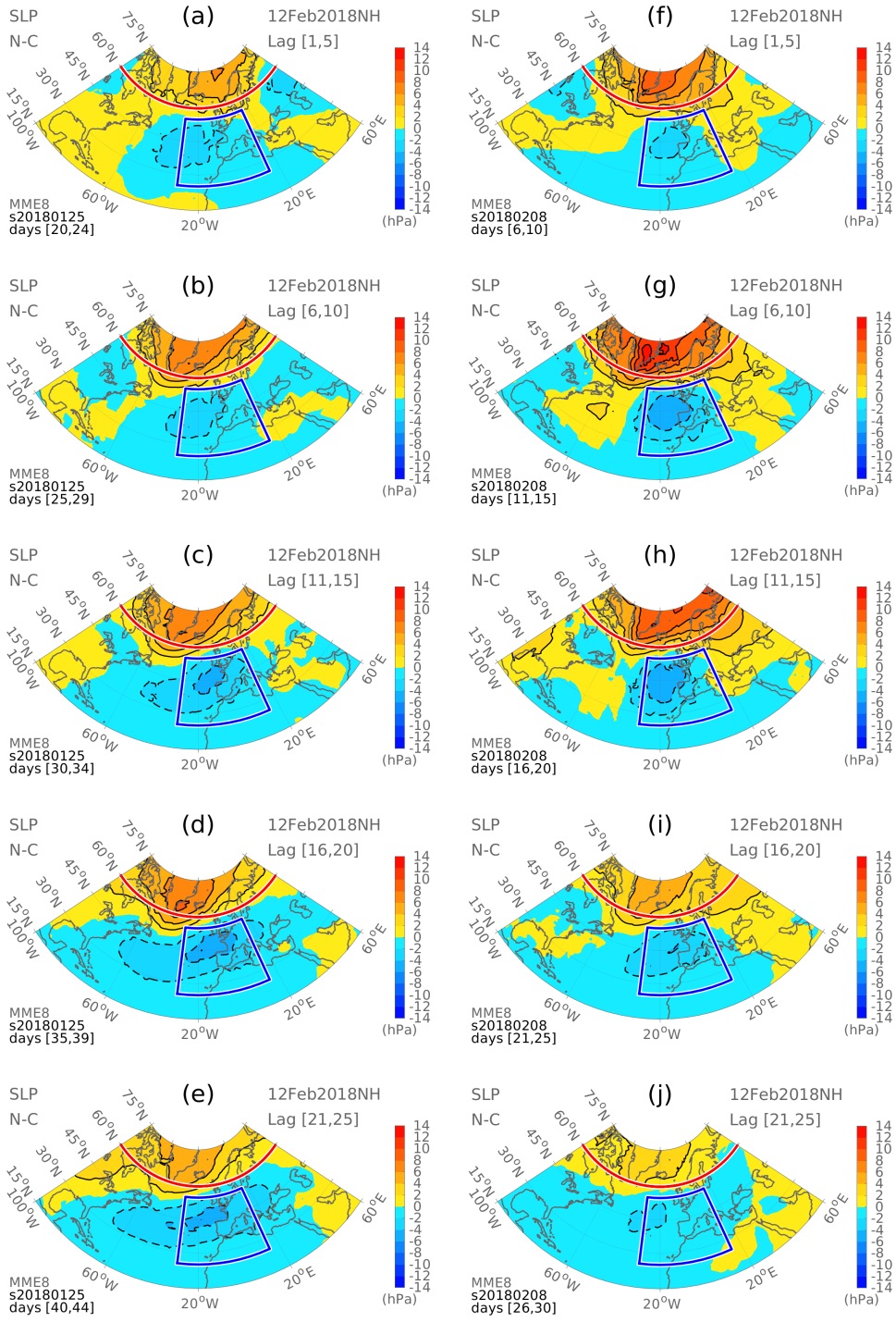

Figure S18. SLP anomalies (shadings) averaged over lag days [1,5], [6,10], [11,15], [16,20], and [21,25] relative to the SSW onset date from the (left) early and (right) late nudged ensemble.

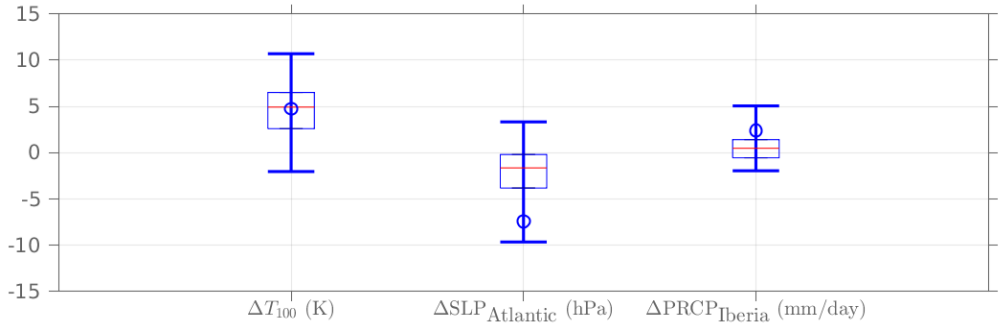

Figure S19. ΔT_{100}, $\Delta\text{SLP}_{\text{Atlantic}}$, and $\Delta\text{PRCP}_{\text{Iberia}}$ for 46 historical SSW events from ERA5. On each box, the red line is the median, the edges of the box are the 25th and 75th percentiles, and the whiskers extend to the most extreme data value. The blue circle indicates the value for the 2018 SSW event.